Disorder-induced splitting of a matter wavepacket in a two-component weakly interacting quantum gas

Guodong Cui (崔国栋)[1,2], Yafan Duan (段亚凡)[1,2], Jianfang Sun (孙剑芳)[1,2], Jun Qian (钱 军)[1,2*], Tao Hong (洪 涛)[3], and Yuzhu Wang (王育竹)[1,2]**

[1] *Key Laboratory for Quantum Optics, Shanghai Institute of Optics and Fine Mechanics, Chinese Academy of Sciences, Shanghai 201800, China*

[2] *Center for Cold Atom Physics, Chinese Academy of Sciences, Shanghai 201203, China*

[3] *Center for Macroscopic Quantum Phenomena, Shanghai Advanced Research Institute, Chinese Academy of Sciences, Shanghai 201203, China*

[*] *Corresponding author: jqian@mail.siom.ac.cn;* [**] *corresponding author: yzwang@mail.shcnc.ac.cn*

Received April 27, 2012; accepted September 4, 2012; posted online December 28, 2011

We theoretically investigate quantum transport of a two-component quantum gas in a disordered potential and predict a unique disorder-induced splitting of a matter wavepacket. We also demonstrate that the splitting of the mobile component originates from the inter-component interaction and the disordered potential on the localized component.

OCIS codes: 020.0020, 020.1475.
doi: 10.3788/COL201210.S20201.

Anderson localization (AL) is a ubiquitous interference phenomenon in which wave cannot propagate in disordered media[1]. After predicted by Anderson in 1958, AL has been reported in classic waves: light in diffusive media[2,3] and photonic crystals[4,5], microwaves[6], and sound waves[7]. Somewhat unexpected, new approaches to the issue came from atomic physics. After the milestone of observing AL in a non-interacting matter wave[8,9], it has been experimentally studied in weak/strong interacting Boson and Fermi gases[2,10]. In the context of disordered quantum gases, controllable disorder can be realized with laser speckles and quasi-periodic lattices[11,12]. Therefore the interplay between disorder and interaction can be investigated in quantum gases with unprecedented versatility, tunability, and measurement possibilities[13].

Nowadays, technique for producing a binary Bose-Einstein condensate (bBEC) is mature and easy which could be two different hyperfine states of the same species[14] or two different species[15]. Since inter-component interaction is introduced and has a great influence on the dynamics of matter wave, a bBEC exhibits more novel dynamical features and macroscopic quantum phenomena in contrast to a conventional BEC which has already attracted intensive studies theoretically and experimentally[16,17]. Depending on interaction strength, the bBEC's ground structure can be divided into miscible and immiscible regimes[18]. Using magnetic or optical Feshbach resonance, people can precisely control scattering length between atoms which can be tuned to from the non-interaction regime to the strong-correlated regimes[19,20].

In this letter, we investigate the long-time transport dynamics of a two-flavor cigar-shaped BEC in one dimension (1D), which is produced in a harmonic oscillator (HO) trap and then is released to expand in a disordered potential. We pay special attention to the situation that the localized and mobile components coexist. It means that one component of the mixture is localized by a quasi-periodic lattice (QPL) acted as disorder, and the other is affected indirectly by disorder due to the interaction between localized and mobile atoms. We numerically solve coupled Gross-Pitaevskii (G-P) equations by split-step Fourier spectral method to observe BEC's dynamical behavior. The strength of disorder is strong enough to ensure that AL of the component A emerges in a short time. Then we find that the density profile of the mobile component B shows a remarkable splitting in coordinate space, which should exhibit a ballistic expansion in the absence of disorder.

Now we begin to introduce theoretical model and discuss numerical results. For simplicity, we assume that a BEC of two different hyperfine states of the same species trapped in the same cylindrical symmetry trap with transverse and axial trap frequencies $\omega_x = \omega_y = \omega_\perp \gg \omega_z$[5]. The QPL plays a role as disorder, and is formed by two lattices superimposing containing a primary lattice whose wave vector is k_1 perturbed by a secondary one k_2, and thus the QPL potential can be expressed as $V'_{\rm QPL} = s_1 E_{\rm R} \sin^2(k_1 z) + s_2 \beta^2 E_{\rm R} \sin^2(\beta k_1 z + \phi)$ with $\beta = \lambda_1/\lambda_2$, where $E_{\rm R} = h^2/(2m\lambda_1^2)$ is the primary lattice's recoil energy, and $s_1 E_{\rm R}$, $s_2\beta^2 E_{\rm R}$ are the lattice depths of the primary and secondary lattices, respectively[21]. The disorder strength can be controlled by the laser intensity of the secondary lattice. By choosing the polarization of the lattice lasers, one can build a state-dependent lattice in which only the component A experiences the QPL potential and the component B is immune from disorder[22]. The bBEC's coupled G-P equation can be derived by minimizing the system's energy at zero-temperature under mean field approximation. The dynamics of the bBEC in 1D can be described by dimensionless coupled G-P equations[23] which are given as

$$\mathrm{i}\frac{\partial \varphi_A}{\partial t} = -\left[\frac{\partial^2}{\partial z^2} + V_{\rm HO} + V_{\rm QPL} + g_{AA}|\varphi_A|^2 + g_{AB}|\varphi_B|^2\right]\varphi_A, \quad (1)$$

$$\mathrm{i}\frac{\partial\varphi_B}{\partial t} = -\left[\frac{\partial^2}{\partial z^2} + V_{\mathrm{HO}} + g_{BB}\left|\varphi_B\right|^2 + g_{AB}\left|\varphi_A\right|^2\right]\varphi_B, \tag{2}$$

with N atoms of each component and the normalization condition $\int_{-\infty}^{+\infty}|\varphi_i|^2\,\mathrm{d}z = 1 (i = A, B)$. $V_{\mathrm{HO}} = \omega_z^2 z^2/2$ is the HO trap potential. The intra-component and inter-component nonlinearity in 1D are given by $g_{ii} = \frac{2k_1 a_{ii}\hbar\omega_\perp N}{E_{\mathrm{R}}}$ and $g_{AB} = \frac{2k_1 a_{AB}\hbar\omega_\perp N}{E_{\mathrm{R}}}$, respectively, where a_{ii} and a_{AB} represent scattering lengths. In the above expressions, the dimensionless units of energy and length are $1/k_1$ and E_{R}, respectively.

Before discussing the main result, we first consider the situation of no inter-component interaction. Under this condition, the dynamics of the bBEC in a disordered potential is easy to understand and the transport dynamics of the component B is trivial. In the AL regime, the QPL has great influence on the wavepacket of the component A and even a complete localization can be observed in a short time. However, the expansion of the wavepacket of the mobile atoms B should not be affected by the presence of disorder due to the absence of the interaction between the localized and mobile atoms, and a ballistic expansion is expected.

Now we turn to discuss the transport of the mobile component in the presence of inter-component interaction and the disordered potential. Numerically, we first obtain ground state of the bBEC in the HO trap using imaginary-time split-step Fourier spectral algorithm. Here, for simplicity, we only consider the miscible case that means the ground-state profiles of both components almost overlap. Then, we abruptly shut off the HO trap to let bBEC diffuse along the axial direction, and the QPL exerted upon the component A is adiabatically loaded. In a long load period, strong disorder strength is favorable to the localization of the component A[24]. The sketch of the transport dynamics is shown in Fig. 1. From now on, nonlinearity coefficients are fixed by $g_{AA} = g_{BB} = g_{AB} = 1$.

First, we check the density profile of the component A between $t = 3\,000$ and $7\,000$ to confirm its localization in the disordered lattice. We find that the density profile is almost unchanged in the long interval, which implies the presence of localization. This can be understood in the context of AL that the disordered potential results

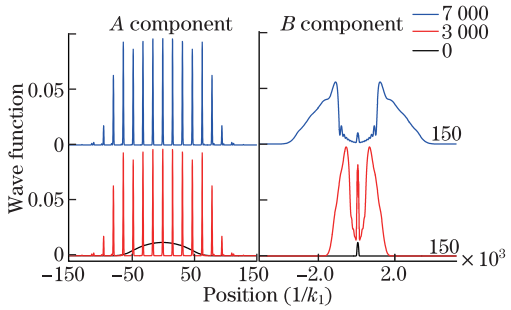

Fig. 1. Transport dynamics of a TBEC in disordered potential. Spatial density profiles of the components A and B at $t = 0$, $3\,000$, $7\,000$ are shown in left and right panels, respectively. The nonlinearity parameters are $g_{AA} = g_{BB} = g_{AB} = 1$. The density profile of the component B is magnified for clarity.

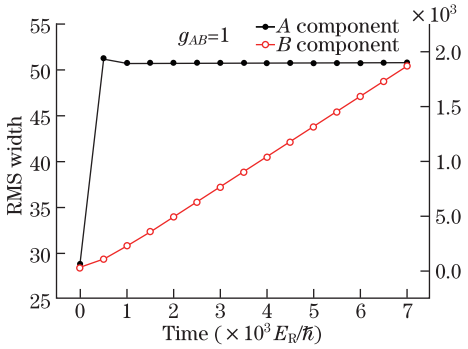

Fig. 2. RMS width of each component of the TBEC during the expansion.

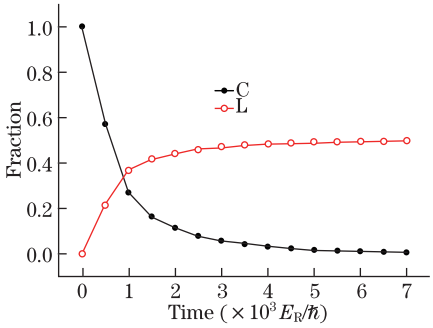

Fig. 3. Fractions of central (solid circle) and left fragments (hollow circle) of the mobile component B.

in coherent multiple scattering of the atomic wavepacket, yielding the wavefunction with absence of diffusion. Furthermore, an interesting phenomenon arises when we turn to observe the dynamics of the mobile component B. An unexpected splitting of matter wave is remarkably exhibited in Fig. 1. Initially the density profile of the component B has an inverse parabola shape. However, new wings toward both sides along the axial direction occur at $t = 3\,000$, which witnesses the splitting of matter wave directly. The symmetric split wings show a two-hump structure and they continue to separate from each other, which is greatly obvious when we compare the density profiles at $t = 3\,000$ and $7\,000$. In addition, the fraction of the central fragment decreases in the propagation while the fraction of new-born wings increases simultaneously. We explain this phenomenon as follows. Since the atoms A are localized in the center region due to the disordered QPL, the repulsive interaction between the atoms push the mobile atoms out of the center zone which can be seen directly from the depletion of the central fragment of the atoms B (see Fig. 1, right panel). Therefore the splitting is a consequence of disorder-induced localization assisted by inter-component interaction.

To further investigate physical mechanism of the splitting, we also calculate root-mean-square (RMS) size of both components of the bBEC (see Fig. 2). Here the RMS size is an important indicative parameter that characterizes the spread of the wavepacket[25]. One can find that the RMS size of the component A increases in a short time of 500 and is nearly fixed thereafter. It is well agreed with the observation for the density profile. On the other hand, the RMS size of the component B always increases which implies the diffusion of its wavepacket. A more direct evidence of the splitting of the mobile

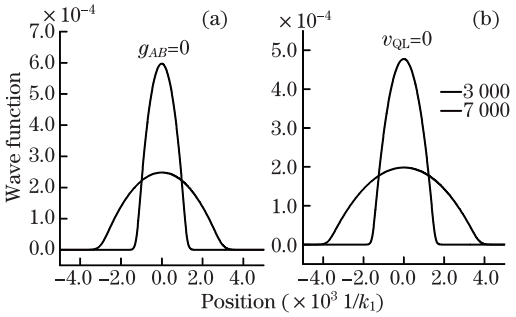

Fig. 4. Density profiles of the component B in coordinate space at $t = 3\,000$ and $7\,000$. (a) $g_{AA} = g_{BB} = 1$ and $g_{AB} = 0$; (b) no QPL and $g_{AA} = g_{BB} = g_{AB} = 1$.

atoms can be seen from the fraction of the center and edge fragments in Fig. 3. The fraction of the center part goes down quickly and the atoms are transferred to the new-born wings. The wings grow up until the depletion of the central fragment. Moreover, the peak of the wing moves outwards which exhibits a visible separation.

It is previously mentioned that a novel splitting of the mobile atoms in the bBEC was observed in numerical simulation. We attribute the splitting of the wavepacket to the coexistence of the inter-component interaction and the localized component due to disorder. In order to shed light on this unexpected splitting, we consider two expansion processes in which only one of the interaction between both components and disorder-induced localization is satisfied. The density profiles of the component B in the two cases are shown in Fig. 4. Only conventional spread of the wavepacket appears, and there is no splitting in both situations. In the former case, as we have discussed briefly, when the interaction between the mobile and localized atoms is absent, the transport of the mobile atoms cannot be affected and the normal diffusion in free space is expected. In the latter case, the absence of disorder cannot lead to the localization of the atoms and both species spread freely after shutting off the trap. The Gaussian-like shape of the wavepacket results from very weakly interaction between the atoms.

Finally, we briefly discuss the experimental realization of the above proposal. First, one can produce the bBEC, and then let one component expand in a 1D QPL which is loaded adiabatically. The binary BEC with different hyperfine sates of ^{87}Rb[14] or two-species mixture of ^{87}Rb-^{41}K[15] have been achieved in the laboratory. Then the state-dependent lattice[22] or species-selective dipole potential[26] irradiates on the BEC in the axis direction. Moreover, the inter-atom interaction can be controlled precisely by Feshbach resonance technique. The dynamics of the condensate can be recorded by *in su* imaging technique. Therefore the proposal is feasible with the state of the art in experiments.

In conclusion, we numerically investigate the transport of the bBEC in the QPL and predicted an intriguing disorder-induced splitting of the mobile wavepacket for the first time. This splitting of matter wave has an evident dependence on the disorder-induced localization and interaction between the localized and mobile atoms. We believe that the present results are of great importance for new insights of quantum transport in disordered quantum gases and more interesting phenomena are expected in the strong-correlated regime.

This work was supported by the National Basic Research Program of China (No. 2011CB921504), the National Natural Science Foundation of China (No. 10974211 and 11104292), and the Research Project of Shanghai Science and Technology Commission (No. 09DJ1400700).

References

1. P. W. Anderson, Phy. Rev. **109,** 1492 (1958).
2. Diederik S. Wiersma, P. Bartolini, A. Lagendijk, and R. Righini, Nature **390,** 671 (1997).
3. M. Stözer, P. Gross, C. M. Aegerter, and G. Maret, Phys. Rev. Lett. **96,** 063904 (2006).
4. T. Schwartz, G. Bartal, S. Fishman, and M. Segev, Nature **446,** 52 (2007).
5. Y. Lahini, A. Avidan, F. Pozzi, M. Sorel, R. Morandotti, D. N. Christodoulides, and Y. Silberberg, Phys. Rev. Lett. **100,** 013906 (2008).
6. A. A. Chabanov, M. Stoytchev and A. Z. Genack, Nature **404,** 850 (2000).
7. H. Hu, A. Strybulevych, S. E. Skipetrov, B. A. van Tiggelen, and J. H. Page, Nature Phys. **4,** 945 (2008)
8. G. Roati, C. D'Errico, L. Fallani, M. Fattor, C. Fort, M. Zaccanti, G. Modugno, M. Modugn, and M. Ingusci, Nature **453,** 895 (2008).
9. J. Bill, V. Joss, Z. Zu, A. Bernard, B. Hambrecht, P. Lugan, D. Cléent, L. Sanchez-Palencia, P. Bouyer, and A. Aspect, Nature **453,** 891 (2008).
10. M. White, M. Pasienski, D. McKay, S. Q. Zhou, D. Ceperley, and B. DeMarco, Phys. Rev. Lett. **102,** 055301 (2009).
11. L. Fallani, J. E. Lye, V. Guarrera, C. Fort, and M. Inguscio, Phys. Rev. Lett. **98,** 130404 (2007).
12. J. E. Lye, L. Fallani, M. Modugno, D. S. Wiersma, C. Fort, and M. Inguscio, Phys. Rev. Lett. **95,** 070401 (2005).
13. L. Sanchez-Palencia and M. Lewenstein, Nat Phys. **6,** 87 (2010).
14. C. J. Myatt, E. A. Burt, R. W. Ghrist, E. A. Cornell, and C. E. Wieman, Phys. Rev. Lett. **78,** 586 (1997).
15. G. Thalhammer, G. Barontini, L. De Sarlo, J. Catani, F. Minardi, and M. Inguscio, Phys. Rev. Lett. **100,** 210402 (2008).
16. S. B. Papp, J. M. Pino, and C. E. Wieman, Phys. Rev. Lett. **101,** 040402 (2008).
17. H. Pu and N. P. Bigelow, Phys. Rev. Lett. **8,** 1134 (1998).
18. H. Pu and N. P. Bigelow, Phys. Rev. Lett. **80,** 1130 (1998).
19. G. Roati, M. Zaccanti, C. D'Errico, J. Catani, M. Modugno, A. Simoni, M. Inguscio, and G. Modugno, Phys. Rev. Lett. **99,** 010403 (2007).
20. R. Yamazaki, S. Taie, S. Sugawa, and Y. Takahashi, Phys. Rev. Lett. **105,** 050405 (2010).
21. M. Modugno, New J. Phys. **11,** 033023 (2009).
22. B. Gadway, D. Pertot, R. Reimann, and D. Schneble, Phys. Rev. Lett. **105,** 045303 (2010).
23. K. Kasamatsu and M. Tsubota, Phys. Rev. A **74,** 013617 (2006).
24. Z. Xu, Y. F. Duan, S. Y. Zhou, T. Hong, and Y. Z. Wang, Chin. Phys. Lett. **26,** 090303 (2009).
25. Y. F. Duan, Z. Xu, J. Qian, J. F. Sun, B. N. Jiang, and T. Hong, Chin. Phys. Lett. **28,** 100302 (2011).
26. J. Catani, G. Lamporesi, D. Naik, M. Gring, M. Inguscio, F. Minardi, A. Kantian, and T. Giamarchi, Phys. Rev. A **85,** 023623 (2012).